

# Design and Analysis of a Wearable Robotic Forearm

Vighnesh Vatsal and Guy Hoffman

**Abstract**—This paper presents the design of a wearable robotic forearm for close-range human-robot collaboration. The robot’s function is to serve as a lightweight supernumerary third arm for shared workspace activities. We present a functional prototype resulting from an iterative design process including several user studies. An analysis of the robot’s kinematics shows an increase in reachable workspace by 246% compared to the natural human reach. The robot’s degrees of freedom and range of motion support a variety of usage scenarios with the robot as a collaborative tool, including self-handovers, fetching objects while the human’s hands are occupied, assisting human-human collaboration, and stabilizing an object. We analyze the bio-mechanical loads for these scenarios and find that the design is able to operate within human ergonomic wear limits. We then report on a pilot human-robot interaction study that indicates robot autonomy is more task-time efficient and preferred by users when compared to direct voice-control. These results suggest that the design presented here is a promising configuration for a lightweight wearable robotic augmentation device, and can serve as a basis for further research into human-wearable collaboration.

## I. INTRODUCTION

Robotic body extensions can augment the abilities of a human wearer, enhance the productivity and safety of workers, and expand the range of activities that people can do in their personal lives. For example, using robotic body extensions, a person can lift more weight, perform repetitive actions with less physical and cognitive load, self-balance in more diverse postures, manipulate hot or toxic objects, position tools more accurately, and reach further than their body’s natural limits. Such wearable robots have been increasingly studied in the form of prostheses, exoskeletons, and supernumerary limbs [1].

In this paper we present the design for a novel configuration of a supernumerary wearable robotic arm intended for close-range human-robot collaboration. Our design is lightweight and attached to the wearer’s elbow, functioning as an additional forearm with a longer range and more degrees of freedom (DoFs) than the human forearm (Fig. 1). We describe the design goals for the robot and present a fully realized prototype based on an iterative design process including several user studies. The resulting robot enhances a user’s reachable workspace, supports picking up objects while both hands are occupied, enables self-handovers, can assist human-human handovers, and provides object stabilization. The robot can perform all of these actions while remaining within the limits of recommended bio-mechanical load on the user, as well as the peak torque capacities of

The authors are with the Sibley School of Mechanical and Aerospace Engineering, Cornell University, Ithaca, NY 14850 USA (e-mail: vv94@cornell.edu; hoffman@cornell.edu)



Fig. 1. Usage scenarios for the wearable robotic forearm design presented in this paper (from top-left): picking up an object with both hands occupied, one-handed self-handover, assisted human-human handover, and stabilizing an object for bi-manual manipulation.

lightweight servo motors. We analyze these performance measures in a number of indicative usage scenarios. In a pilot study, we also explore user preferences regarding the level of autonomy desirable in the robot. Our findings suggest that the proposed configuration is a promising design for human-wearable-robot collaboration.

### A. Related Work

Traditionally, most efforts in wearable robotics have focused on prostheses and exoskeletons, reaching considerable maturity in both research and commercialization. Robotic prostheses generally serve as replacements for lost human functionality [2], [3]. Exoskeletons are worn in addition to existing human limbs [4], and serve in one of two roles: in parallel with unhealthy joints for support or rehabilitation [5], or to augment and enhance healthy human limbs in functions such as walking or lifting loads [6], [7]. For two recent surveys on robotic body augmentations, see: [8], [1].

In contrast to these two kinds of wearable robots, we are now also witnessing the development of robotic augmentations for able-bodied persons in the form of supernumerary limbs, such as the one described in this paper. These are not restricted to replace or support human limbs, but instead add

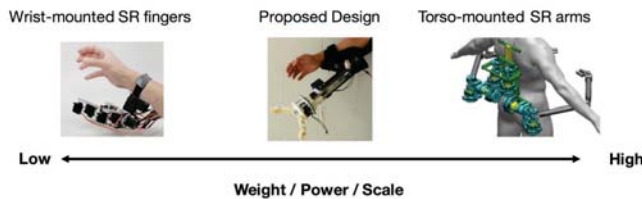


Fig. 2. The proposed design falls in between existing supernumerary robotic (SR) limb designs (wrist-mounted SR fingers [15] and torso-mounted SR arms [9]) in terms of weight, power, and scale.

DoFs that are not present in the human body.

One such example is a torso-mounted pair of robotic arms for use in aircraft manufacturing and for bracing to support a crouching worker [9], [10]. These are super-human sized robots capable of up to 50–70 Nm of torque. A lighter version of these arms was developed to hold a workpiece in place and enable the wearer to screw it into position [11]. A similarly structured shoulder-worn arm was recently presented in a drumming application [12].

On the lower end of the size and weight spectrum are wrist-mounted robotic fingers designed to perform two-handed tasks with a single hand [13], [14], [15]. A similar design was used as a rehabilitation tool for patients with limited functionality in one hand [16], and another as a dynamically adjusting interface or haptic joystick for on-screen control [15], [17]. These are low-power, lightweight devices with limited reach, akin to supernumerary fingers.

The wearable robotics configurations described above represent two extremes in terms of application, mounting point, size, weight, and power.

### B. Contribution and Overview

The design we present in this paper falls in between these two extremes (Fig. 2). It is a lightweight device for shared autonomy in general human-robot collaboration settings. Specifically, we present a human-scale wearable robotic forearm, attached at the elbow. Our design is aimed at tasks with lower demands than the torso-mounted robots described above, leading to significantly less powerful motors and a smaller footprint and weight. At the same time, we are seeking a configuration that allows for extended reach and multi-location work capabilities, in contrast to wrist-worn robotic fingers.

We envision the robot functioning as a general-purpose autonomous collaborative agent working in tight synchrony with human activities, and sharing the workspace with them. The presented design is part of a research project aimed at developing autonomous control methods for collaborative wearable robotics.

This novel configuration presents technical challenges in design, control, and human-robot interaction. In this paper, we focus primarily on the design and interaction aspects of the arm, as follows: Section II describes the design goals of the arm, and the resulting development of two iterative models. Section III analyzes the workspace volume enhancement while wearing the robotic arm. Section IV evaluates

the robotic arm in terms of the bio-mechanical loads on the wearer and torque loads on the actuators in a number of indicative usage scenarios. We present a preliminary evaluation of user preferences in interaction modes with the robot, and conclude with future work in Section V.

## II. PHYSICAL DESIGN

### A. Design Goals

The project described herein envisions to provide a collaborative, range-extending forearm that can be worn on the user’s own arm for rapid, close-body human-robot tasks. The proposed device fills the design gap in the state of the art between torso mounted, high powered designs, and low-range wrist-mounted devices. Addressing this gap, we identify the following design goals: (a) The robot should add new capabilities to the wearer, and should extend their operating range. Specifically, it should enable the human and robot to act simultaneously in two locations, and support self-handovers as well as handovers to other humans; (b) The robot should be light and well-balanced enough to be wearable on one’s arm; (c) The robot should be able to operate on the time scales of human manual activities. In the long run, the robot should operate autonomously in a collaborative scenario, with minimal addition to the wearer’s cognitive load.

### B. Model I Prototype

We initially explored a three-DoF design (“Model I”), with a DoF at the elbow for horizontal panning, a prismatic joint for length extension, and a two-fingered gripper as the end effector, shown in Fig. 3. This first prototype was designed with workbench operation in mind, broadening the wearer’s effective “wing span.” It also supported the design goal of working simultaneously at two locations, and that of self-handovers and human-human handovers, allowing two people working side by side to stand further apart from each other.

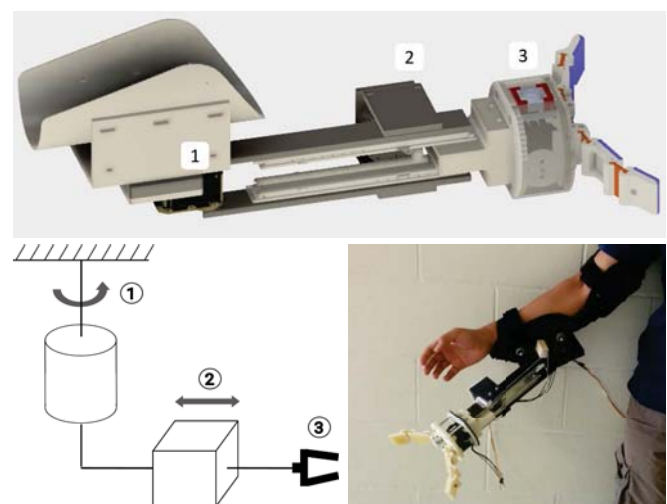


Fig. 3. CAD model, kinematic diagram and physical realization of Model I with three DoFs: 1) Horizontal panning, 2) Length extension, 3) Gripping.

The robot was mounted on an arm brace, and made of laser-cut and 3D printed ABS components and a stainless steel linear slider actuated via a rack-and-pinion drive system. The rotational DoF was direct-driven. The end effector was based on the Yale OpenHand Model T42 [18], adjusted for lower weight by constraining both fingers to move together with a single motor. The arm weighed  $\sim 2$  kg, and was  $\sim 640$  mm in length when not extended. The extension was  $\sim 160$  mm. The panning range about the user's elbow was  $\sim 120^\circ$ . The actuators were one MX-64 and two MX-28 Dynamixel servo motors from ROBOTIS. The prototype was tethered, receiving both power and control commands through cables.

### C. Model I Usability Studies

With this prototype as a platform, we conducted an online survey to discover the usage contexts and functions that people envision for such a device [19]. We found that people consider a third arm to be a functional tool in professional settings, such as assisting in working with power tools, or handling packages in a warehouse.

With this insight, we further conducted a contextual inquiry into the specific professional field of building construction. Following a need-finding protocol [20], we discovered three potential usage contexts for the third arm in construction: reaching and self handovers of objects such as tools while the user cannot move from their spot, stabilization of objects and user's bodies, especially while working in tightly constrained spaces, and coordination in collaborative activities such as putting up drywall, which normally require two people to work in tandem.

Finally, to evaluate Model I's design, we conducted an in-lab usability study, collecting feedback from people while they interacted with the device. We also sought to identify areas for improvement in the design. Participants wore the device and performed a pick-and-place maneuver, and a two-person handover. The full description of these studies is presented in [19], and only the main design-related results are described here. We found that users were concerned with the device's weight and limited range, and the need to precisely place the gripper around the object to be handled. The robot was also found to be slow to extend and retract. Overall, users wanted a more lightweight and dexterous device, informing the improvements in the next prototype. Users also wanted a wearable arm that has adjustable autonomy, and can communicate its intent. This supports our longer-term goal of a collaborative wearable robot, and is also reflected in the findings from a pilot study detailed in Section V-B.

### D. Model II

As described in the previous section, the main design shortcomings of Model I were its weight, limited dexterity with respect to grasping angle, and the speed of the prismatic joint.

To address these concerns, we added two additional DoFs to the redesigned arm ("Model II"): a vertical pitching of the arm (MX-64 Dynamixel), and a wrist rotation before the

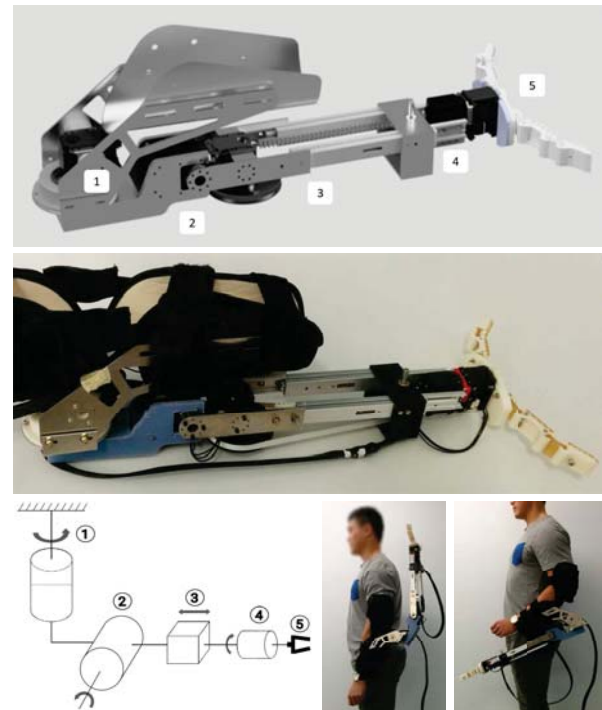


Fig. 4. CAD model, kinematic diagram and physical implementation of the Model II prototype with two additional degrees of freedom, for a total of five: 1) Horizontal Panning, 2) Vertical pitching, 3) Length extension, 4) Wrist Rotation, 5) Gripping.

gripper (AX-12 Dynamixel) (Fig. 4). The vertical pitching, along with complete  $360^\circ$  panning, results in a full 3D workspace (Fig. 5), and allows the user to reach objects placed below as well as behind the user. In contrast, the workspace in Model I was constrained to a planar region with respect to the wearer's arm. Furthermore, to allow for rapid motion of the linear DoF we added a 1:7 transmission ratio between the motor and the pinion gear in the rack and pinion assembly on the linear sliders.

To address weight considerations, we replaced most of the ABS components with waterjet-machined sheet aluminum parts, and used lightweight aluminum linear sliders instead of the stainless steel ones in Model I. We also redesigned the gripper, in particular the attachment points to the linear rail, greatly reducing its size and weight. Finally, we re-positioned the motors behind the elbow for a more balanced weight distribution. Overall, even after adding two more DoFs and a transmission system, we were able to achieve a weight reduction by  $\sim 0.5$ kg compared to Model I.

### E. Evaluation

We evaluate the improvement in Model II compared with Model I in a scenario that can be performed by both devices, using the load analysis method discussed in detail in Section IV below. The scenario is to grasp an object that is just out of reach while seated at a desk (Fig. 6 left), with the following steps: *Pan outwards to  $+60^\circ$*   $\rightarrow$  *Fully extend arm*  $\rightarrow$  *Grip*  $\rightarrow$  *Pan inwards to  $-60^\circ$*   $\rightarrow$  *Open gripper*. We find that the magnitudes of moments experienced by the wearer at their elbow and shoulder are reduced by 18 to 35% for

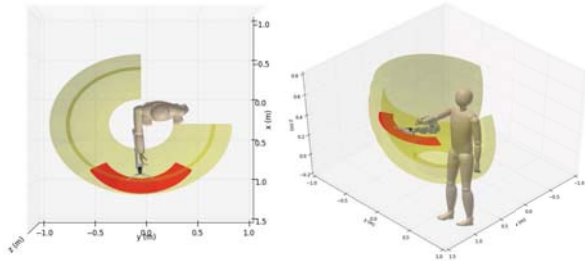


Fig. 5. Model II offers a larger, full 3D workspace (yellow) compared to Model I (red) for the same fixed body configuration of the user.

Model II compared to Model I (Fig. 6).

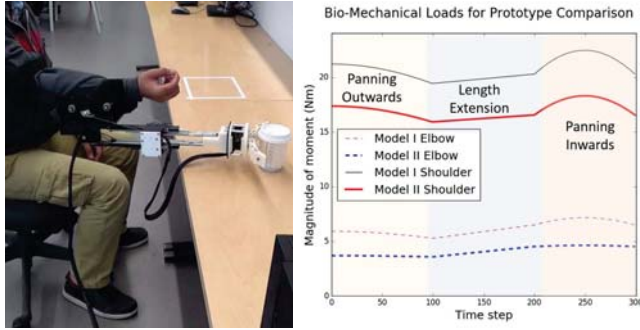


Fig. 6. In a task involving moving an object across a table, Model II exerts a moment load at the user's shoulder and elbow that is 18–35% lower than Model I.

### III. WORKSPACE ANALYSIS

To quantify the workspace enhancement of the proposed human-wearable robot configuration with respect to the workspace afforded by the natural human body, we employ a combined human-robot model (Fig. 7). Generally, the human arm can be represented as a 7-DoF serial chain [4]. However, since we are only interested in measuring its workspace volume, we can combine the wrist and forearm into a single rigid link and use a reduced 5-DoF model. The robotic arm is represented as a serial chain concatenated to the human arm, forming a combined 9-DoF human-robot model, excluding the gripper.

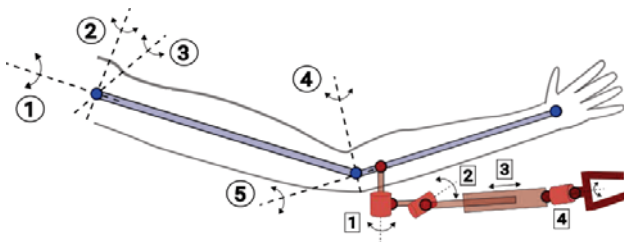


Fig. 7. Schematic used in the workspace analysis of a human arm with the robotic arm attached at the elbow, illustrating the DoFs in Tables I and II.

The kinematics of each of these serial chains are described with coordinate frames derived using the Denavit-Hartenberg (D-H) convention [21]. The D-H parameters allow us to construct a  $4 \times 4$  homogeneous transformation matrix  $T_0^n$

between the coordinate frame at the origin (glenohumeral joint) and the frame at the end-effector, using (1), where  $n = 5$  is the number of joints. In Table I, the parameters  $a_3$  and  $d_5$  corresponding to anthropometric data, and  $\theta_i$ , the joint ranges of motion, have been adapted from [4] and the NASA Man-System Integration Standards [22].

$$T_0^n = \prod_{i=1}^n T_{i-1}^i(\alpha_i, a_i, d_i, \theta_i) \quad (1)$$

TABLE I

D-H PARAMETERS FOR THE 5-DOF HUMAN ARM MODEL

Degree of Freedom	$\alpha_i$	$a_i$ (m)	$d_i$ (m)	$\theta_i$
1) Shoulder circumduction	$-90^\circ$	0	0	$[0^\circ, 180^\circ]$
2) Shoulder adduction	$+90^\circ$	0	0	$[-90^\circ, 140^\circ]$
3) Shoulder flexion	$0^\circ$	0.335	0	$[-90^\circ, 170^\circ]$
4) Elbow flexion	$+90^\circ$	0	0	$[80^\circ, 235^\circ]$
5) Elbow pronation	$+90^\circ$	0	0.263	$[0^\circ, 180^\circ]$

TABLE II

D-H PARAMETERS FOR THE WEARABLE ROBOTIC ARM

Degree of Freedom	$\alpha_i$	$a_i$ (m)	$d_i$ (m)	$\theta_i$
1) Horizontal panning	$+90^\circ$	-0.112	0	$[-180^\circ, 180^\circ]$
2) Vertical pitching	$+90^\circ$	0	0	$[-180^\circ, 30^\circ]$
3) Length extension	$0^\circ$	0	$[0.28, 0.44]$	$180^\circ$
4) Wrist rotation	$0^\circ$	0	0.106	$[-180^\circ, 180^\circ]$

Similar to (1), we can construct a transformation matrix  $P_0^m$  using the D-H parameters for the robot (Table II), and concatenate it with  $T_0^n$  to get the transformation matrix  $S_0^{n+m}$  for the combined human-robot model, as shown in (2). To account for the attachment point offset between the human and robot, parameters for the fifth DoF in  $T_0^n$  need to be modified to  $a_5 = 0.075$  m,  $d_5 = 0.016$  m.

$$S_0^{n+m} = \prod_{i=1}^n T_{i-1}^i \prod_{j=1}^m P_{j-1}^j \quad (2)$$

#### A. Workspace Computation Results

The total reachable workspace volume is the union of workspaces generated when a mechanism undergoes its full range of motion (RoM). It is estimated using a Monte-Carlo sampling procedure as proposed in [23]. Each joint variable,  $\theta_i$  or  $d_i$  is drawn from a Beta random distribution,  $\theta_i, d_i \sim \text{Beta}(\alpha, \beta)$ , where the distribution parameters  $\alpha$  and  $\beta$  are determined based on the RoM for each DoF. This reduces the sparsity of points at the ends of the joint space range. We use the full RoMs for both serial chains in (1) and (2) to obtain the sets of points in 3D, that constitute the total reachable workspace volumes of the human arm model and combined human-robot model respectively. To compute the volume, these point clouds are sectioned into 2D slices along the  $Z$ -axis, and numerically integrated using a trapezoidal method:

$$V = h \left[ \sum_{i=1}^s A_i - \frac{1}{2}(A_1 + A_s) \right] \quad (3)$$

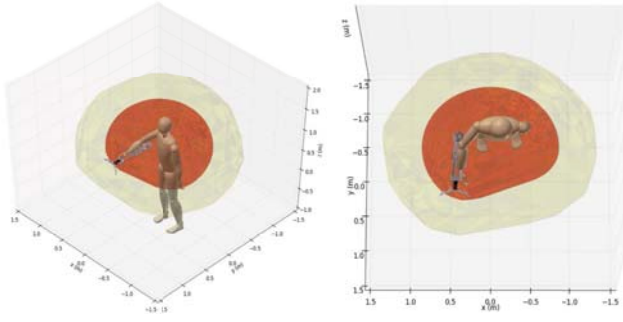


Fig. 8. Convex hulls of the workspace point clouds illustrating the improvement in total reachable workspace afforded by the robotic arm (yellow) over the natural human arm range (red).

Here  $h = [z_{max} - z_{min}] / s$  is the step size with  $s$  steps, and  $A_i$  is the area of the  $i^{\text{th}}$  slice. The simulations are performed using a Unified Robot Description Format (URDF) [24] model of the robotic arm and an articular 34-DoF model of the human body, adapted from [25]. The total reachable workspace volume is enhanced from 1.003 m<sup>3</sup> for the human arm alone, to 3.467 m<sup>3</sup> while wearing the robotic arm, an increase of 246%, illustrated in Fig. 8.

#### IV. EVALUATION OF OPERATING LOADS

For a person to wear the robot for prolonged periods of time, we need to consider the bio-mechanical load on the wearer. In this section, we evaluate these loads for the Model II prototype. There is a direct trade-off between a low bio-mechanical load, and adequate power density in the actuators for rapid collaborative action. Therefore, we also provide an analysis of the torque requirements on the robot's motors.

##### A. Usage Scenarios

We use three indicative collaborative scenarios based on the design goals and user study findings discussed in Sections I and II-C: fetching an object from below the human's workspace for self-handover; human-to-human handover assisted by the robotic arm; and fixing an object in position while the human is operating on it (Fig. 1).

*a) Fetching from Below:* This task involves a combination of horizontal panning, pitching down, and length extension to reach the object to be fetched. Once the object is grasped, it is brought over to the user's own hands.

*b) Assisted Human-Human Handover:* In this scenario, two humans are working back to back. The wearer has an object within their workspace that they want to transfer to another person while their own hands or attention are occupied. The robot grasps the object and hands it over to a person standing behind the user by panning outwards.

*c) Fixing an Object in Position:* This scenario does not involve moving an object, but focuses on the robot stabilizing both itself and an object, for example holding a block of wood in place while the user drills into it.

##### B. Bio-Mechanical Load Analysis

To evaluate the bio-mechanical load on the user in these scenarios, we model the human-robot system as two distinct

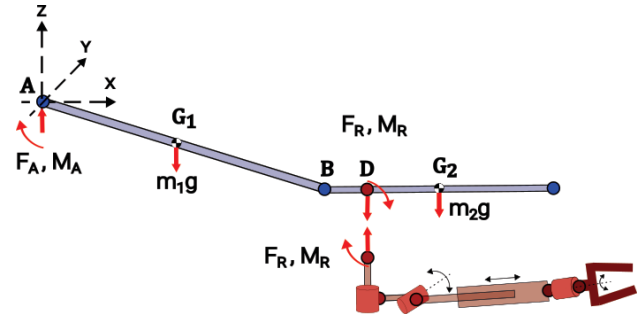


Fig. 9. Free-body diagram of the human arm with the robot as a point load and moment.

bodies, as shown in Fig. 9. The interaction between the robot and the human arm takes the form of the support force  $\vec{F}_R$  and moment  $\vec{M}_R$ .

For each trajectory,  $\vec{F}_R$  and  $\vec{M}_R$  are computed using the iterative Newton-Euler dynamics algorithm [26] applied to the robot. As shown in Fig. 7, the robot is considered to be a 4-DoF model with 5 links. For each task trajectory, the motors are assumed to rotate at constant angular speeds during the motions. The ramping up and down of angular velocities during the start and end of a trajectory, as well as sign changes during a trajectory, are assumed to be nearly instantaneous, taking between two and five time steps. The resulting accelerations of the links, and forces and moments at the joints are computed iteratively, going from link 1 to link 5, with a different reference frame attached to each link. The outward iteration equations below provide the linear acceleration  $\dot{v}$  and angular acceleration  $\dot{\omega}$  of link  $i + 1$ , given these quantities for link  $i$ . The matrix  $R_i^{i+1}$  is the transformation between frames attached to link  $i + 1$  and link  $i$ .  $\theta_i$  is the joint angle for each motor,  $d_i$  is the length of the prismatic joint, and  $\hat{z}_i^i$  is the joint axis for joint  $i$  in frame  $i$ .  $P_i^{i+1}$  is the position vector going from the origin of frame  $i$  to the origin of frame  $i + 1$ . The initial conditions for the outward iterations are specified at the ground link (link zero) of the serial chain [27]:  $\omega_0^0 = 0$ ,  $v_0^0 = 0$ ,  $\dot{\omega}_0^0 = 0$  and  $\dot{v}_0^0 = \vec{g}$ , where  $\vec{g}$  is acceleration due to gravity.

$$\omega_{i+1}^{i+1} = R_i^{i+1} \omega_i^i + \dot{\theta}_{i+1} \hat{z}_{i+1}^{i+1} \quad (4)$$

For rotary joints (all except DoF 3):

$$\dot{\omega}_{i+1}^{i+1} = R_i^{i+1} \dot{\omega}_i^i + R_i^{i+1} \omega_i^i \times \dot{\theta}_{i+1} \hat{z}_{i+1}^{i+1} + \ddot{\theta}_{i+1} \hat{z}_{i+1}^{i+1} \quad (5)$$

$$\dot{v}_{i+1}^{i+1} = R_i^{i+1} [\dot{\omega}_i^i \times P_i^{i+1} + \omega_i^i \times (\omega_i^i \times P_i^{i+1}) + \dot{v}_i^i] \quad (6)$$

For DoF 3, which is prismatic:

$$\dot{\omega}_{i+1}^{i+1} = R_i^{i+1} \dot{\omega}_i^i \quad (7)$$

$$\dot{v}_{i+1}^{i+1} = R_i^{i+1} [\dot{\omega}_i^i \times P_i^{i+1} + \omega_i^i \times (\omega_i^i \times P_i^{i+1}) + \dot{v}_i^i] + 2\omega_{i+1}^{i+1} \times \dot{d}_{i+1} \hat{z}_{i+1}^{i+1} + \ddot{d}_{i+1} \hat{z}_{i+1}^{i+1} \quad (8)$$

The linear accelerations  $\dot{v}_{c,i}$  of the centers of mass (COMs) of each link are computed as follows, along with the inertial forces  $F_i$  and moments  $M_i$  on each link.  $P_{c,i}^i$  is the position of the COM of link  $i$  in frame  $i$ , and  $I_{c,i}$  is the moment of inertia about the COM.

$$\dot{v}_{c,i} = \dot{\omega}_i^i \times P_{c,i}^i + \omega_i^i \times (\omega_i^i \times P_{c,i}^i) + \dot{v}_i^i \quad (9)$$

$$F_i = m_i \dot{v}_{c,i} \quad (10)$$

$$M_i = I_{c,i} \dot{\omega}_i^i + \omega_i^i \times (I_{c,i} \omega_i^i) \quad (11)$$

The inward iterations, going from link 5 to link 1, use the above quantities to compute the forces  $f_i^i$  and moments  $n_i^i$  exerted on link  $i$  by link  $i+1$  as seen in frame  $i$ .

$$f_i^i = R_{i+1}^i f_{i+1}^{i+1} + F_i^i \quad (12)$$

$$n_i^i = M_i^i + R_{i+1}^i n_{i+1}^{i+1} + P_{c,i}^i \times F_i^i + P_i^{i+1} \times (R_{i+1}^i f_{i+1}^{i+1}) \quad (13)$$

The initial condition for inward iterations is the external loading at the end-effector of the robot. For the third arm scenarios, we consider the gripper to be holding a plastic cup weighing  $\sim 30$ g, giving us  $f_6^6 = -0.29\hat{k}$  N,  $n_6^6 = \vec{0}$ . The required interaction loads between the robot and human arm are given by  $\vec{F}_R = f_0^0$  and  $\vec{M}_R = n_0^0$ .

The human arm remains static during the trajectories in scenarios (a) and (b) of the robot. This allows us to use a simplified static arm model to estimate the bio-mechanical loading. This load consists of the force norms at the human shoulder and elbow:  $\|\vec{F}_A\|$ ,  $\|\vec{F}_B\|$ , and corresponding moment norms:  $\|\vec{M}_A\|$ ,  $\|\vec{M}_B\|$ .

These quantities can be computed for each scenario assuming static equilibrium. Using the notation in Fig. 9,

$$\vec{F}_A = \vec{F}_R + m_1\vec{g} + m_2\vec{g} \quad (14)$$

$$\vec{M}_A = \vec{M}_R + \vec{r}_{G_1/A} \times m_1\vec{g} + \vec{r}_{G_2/A} \times m_2\vec{g} + \vec{r}_{D/A} \times \vec{F}_R \quad (15)$$

$$\vec{F}_B = \vec{F}_R + m_2\vec{g} \quad (16)$$

$$\vec{M}_B = \vec{M}_R + \vec{r}_{G_2/B} \times m_2\vec{g} + \vec{r}_{D/B} \times \vec{F}_R \quad (17)$$

The magnitudes of bio-mechanical forces at the human shoulder and elbow,  $\|\vec{F}_A\|$ , and  $\|\vec{F}_B\|$  remain almost constant in these scenarios, as the centrifugal and Coriolis effects are negligible compared to the weights of the links. The peak force loads are  $\sim 55.8$  N and  $\sim 31.3$  N, at the shoulder and elbow respectively. For comparison, the peak force loads that a human can withstand are  $\sim 100$  to  $500$  N at the shoulder, and  $\sim 50$  to  $400$  N at the elbow, depending on the arm configuration [28].

Fig. 10 shows the bio-mechanical moment loads  $\|\vec{M}_A\|$  and  $\|\vec{M}_B\|$  during scenarios (a) and (b). In both tasks, the object being manipulated is a plastic cup weighing  $\sim 30$  g. The peak moment loads on the wearer's shoulder and elbow during these tasks are  $\sim 24.8$  Nm and  $\sim 11.6$  Nm respectively. For comparison, the human shoulder can withstand moment loads of magnitude  $\sim 85$  to  $130$  Nm, while the elbow can withstand  $\sim 40$  to  $80$  Nm [28], [29]. Bio-mechanical load evaluations are omitted for scenario (c) due to its statically indeterminate nature.

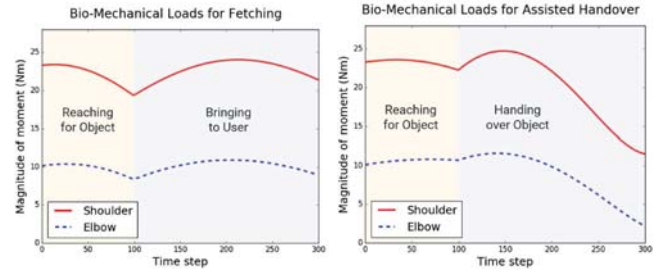


Fig. 10. The bio-mechanical moment loads during the fetching and handover tasks are well within human limits of  $\sim 40$ – $80$  Nm for the elbow and  $\sim 85$ – $130$  Nm for the shoulder.

### C. Motor Torque Loads

We measured motor torque loads directly from the built-in sensors on the servo motors used in our robot. In all three scenarios, non-negligible torque loads are present only in DoFs 1 and 2. In the bracing operation, the wrist and gripper are isolated from the vibration loads of the power screwdriver due to the compliant finger structure.

Fig. 11 shows motor torque loads for all three scenarios. These loads remain below 50% of the motor's peak rating of 6.0 Nm for the first two scenarios, and below 20% for bracing.

To summarize, these evaluations reflect that the improvements in Model II adequately address its major design goals. Our analysis shows that the bio-mechanical loads on the wearer from the robot are well within acceptable limits. Concurrently, the joint motors remain within operating conditions during typical usage scenarios for the third arm.

## V. DISCUSSION AND FUTURE WORK

This paper presents a novel configuration for a wearable robotic forearm, designed for close-range human-robot collaboration. We present two incrementally actualized models that augment the user's reach in shared workspaces. Kinematic analysis shows the reachable workspace increases by 246% compared to the natural human workspace, indicating a consequential increase in reach for a lightweight wearable device. Furthermore, the design's DoFs and wide range of motion support a variety of scenarios identified in usability studies, including picking up objects for self-handovers, assisting in human-human handovers—even behind the wearer's back—and providing object stabilization.

A major design consideration in this configuration is the balance between the functional enhancements provided by the robot and the load on the wearer. We evaluated the performance of the robot with these design goals in mind. We find our design to be low in weight and well-balanced enough to stay within human bio-mechanical force and moment limits throughout the above-mentioned scenarios. In addition, the low motor torque loads we measured suggest the possibility of using even more lightweight motors in subsequent design iterations, further reducing the bio-mechanical load on the wearer.

Apart from the physical design aspect, an important area of exploration is the level of autonomy, and desired mode of interaction between the user and the robot.

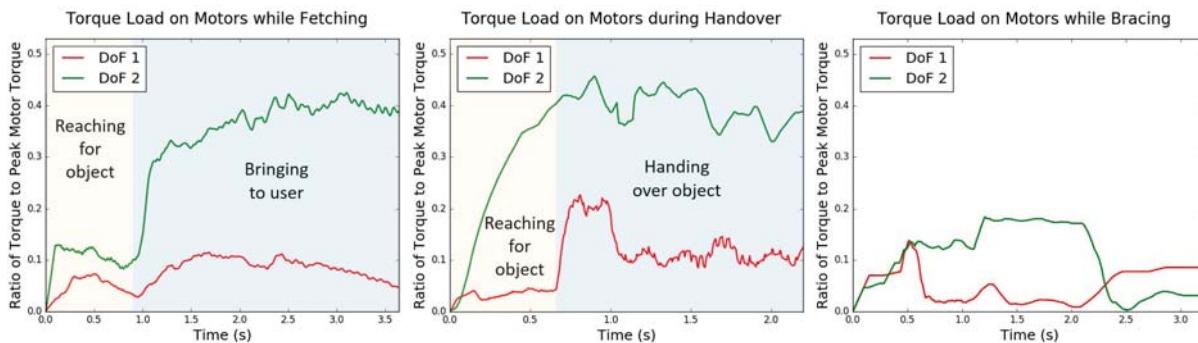


Fig. 11. The torque load on the servo motors used for the panning and vertical pitching DoFs never exceeds 50% of their peak rating of 6.0 Nm

### A. Human-Robot Interaction and Autonomy

The usability study described in section II-C addresses this aspect of human-robot interaction (HRI), collaboration, and autonomy distribution between wearer and robot. From the study, we gained some insights into the control and autonomy desired by users:

- There should be some mode of communication between the human and robot, in the form of visual, haptic, or verbal cues.
- At the same time, the kind of autonomy provided to the robot should reduce cognitive load on the user. The user should not be confused by the robot’s actions.
- Participants expressed interest in being able to give high-level commands verbally, and the robot being able to handle the implementation of those commands autonomously.

This presents a well-known interaction trade-off or gradient between complete autonomy of the robot, and the user giving commands to the robot to complete a given task [30]. To explore this, we conducted a pilot study for a pick-and-place task with the Model II prototype.

### B. Pilot HRI Study

In the study, participants wore the robot and used both of their hands, and the robotic arm for a self-handover task involving two objects, one of which was out of reach (Fig. 12).

They performed the task under two conditions. In one, participants used voice commands (e.g. “left”, “right”, “grasp”) to directly steer the robot. The second interface was presented as an autonomous arm, but was in fact a Wizard-of-Oz (“WoZ”) setup [31] where a remote operator directly controlled the robot’s motion, unbeknownst to the users. Eight participants wore the robotic arm, and completed the same task three times with each interface, counterbalanced for order effects.

The mean completion time was significantly faster and less variable using WoZ (mean  $M_w = 12.97s$ , std. dev.  $S_w = 3.31$ ) compared to the voice interface (mean  $M_v = 24.60s$ , std. dev.  $S_v = 8.79$ ;  $M_v - M_w = 11.64s$ ;  $t(7) = 4.39, p < 0.01, d = 1.55$ , Fig. 12). This suggests that even though participants had no control over the arm’s movement, they were able to complete the task faster. In questionnaires, users

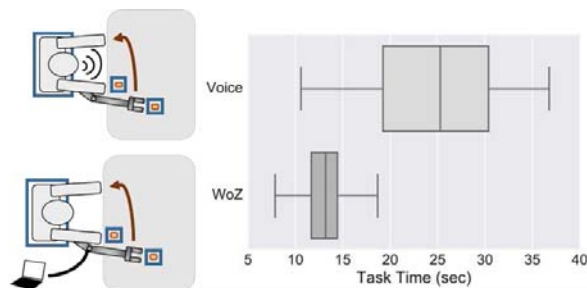


Fig. 12. Setup of the pilot study: the robot brings the orange objects on the table to the user’s other arm. The user and objects are constrained within the blue rectangles, making one object too far for their own arm to reach. The two study conditions are a voice-operated robot (left, top), and a Wizard-of-Oz setup perceived as autonomous by the user (left, bottom). “Autonomous” WoZ behavior of the robotic arm resulted in significantly shorter and less varied task times than direct voice control (right) as well as being preferred by users.

also rated the desirability of the “autonomous” movement higher than the direct voice control. While these are only preliminary results and require more rigorous testing, they indicate that providing a wearable robot with autonomy can reap task efficiency and usability benefits.

### C. Future Work

While this paper addresses the design challenges for the proposed robotic configuration, there are many additional challenges related to the control aspects of a wearable robotic forearm. For example, the robot needs a control method to dynamically adapt to rapid disturbances to its reference frame introduced by the wearer’s arm movements. The appropriate use of a mixture of human body sensors and internal robot sensors to address this control challenge is also an open question.

Autonomy in human wearable-robot collaboration opens the way for many other uncharted research areas. These include planning, action coordination, fluency, and safety concerns of a wearable autonomous robot. The constraints and parameters of human-wearable collaboration are decidedly different from traditional human-robot collaboration, where the robot and human are separate agents. This raises

some interesting questions: Can the robot make use of the wearer's movement to achieve its goals? How can it integrate beliefs over future movements of the wearer to adapt its plan? How can it communicate its goals without putting more cognitive load on the wearer? And how can this collaborative behavior be carried out in a safe fashion, given the close proximity to the human?

Usability and ergonomics aspects, such as fatigue, habituation, and learning curves are also important research questions that need to be addressed before such a robot can be made widely accessible. And finally, there are interesting research questions surrounding the wearer's proprioception, and perception of autonomy vis-à-vis a collaborative robot attached to their own body.

We believe that the robot presented here offers a promising platform to explore these open research questions.

#### ACKNOWLEDGMENTS

This material is based upon work supported by the National Science Foundation under NRI Award no. 1734399. We thank Siyu Zhou for assistance with the prototype's physical design, and him and Harrison Chang for conducting the interaction pilot study.

#### REFERENCES

- [1] M. Bergamasco and H. Herr, "Human-robot augmentation," in *Springer Handbook of Robotics*. Springer, 2016, pp. 1875–1906.
- [2] J. T. Belter and J. L. Segil, "Mechanical design and performance specifications of anthropomorphic prosthetic hands: a review," *J. of Rehabilitation Res. and Develop.*, vol. 50, no. 5, p. 599, 2013.
- [3] B. E. Lawson, J. Mitchell, D. Truex, A. Shultz, E. Ledoux, and M. Goldfarb, "A robotic leg prosthesis: Design, control, and implementation," *IEEE Robotics Automation Magazine*, vol. 21, no. 4, pp. 70–81, Dec 2014.
- [4] J. L. Pons, *Wearable robots: biomechatronic exoskeletons*. John Wiley & Sons, 2008.
- [5] R. Gopura and K. Kiguchi, "Mechanical designs of active upper-limb exoskeleton robots: State-of-the-art and design difficulties," in *ICORR 2009. IEEE Int. Conf.*, pp. 178–187.
- [6] J. E. Pratt, B. T. Krupp, C. J. Morse, and S. H. Collins, "The roboknee: an exoskeleton for enhancing strength and endurance during walking," in *Robotics and Automation (ICRA), 2004 IEEE Int. Conf.*, vol. 3, pp. 2430–2435.
- [7] A. M. Dollar and H. Herr, "Lower extremity exoskeletons and active orthoses: challenges and state-of-the-art," *IEEE Trans. Robot.*, vol. 24, no. 1, pp. 144–158, 2008.
- [8] T. Yan, M. Cempini, C. M. Oddo, and N. Vitiello, "Review of assistive strategies in powered lower-limb orthoses and exoskeletons," *Robotics and Autonomous Syst.*, vol. 64, pp. 120–136, 2015.
- [9] C. Davenport, F. Parretti, and H. H. Asada, "Design and biomechanical analysis of supernumerary robotic limbs," in *ASME 2012 5th Annu. Dynamic Systems and Control Conf.*, pp. 787–793.
- [10] F. Parretti and H. H. Asada, "Supernumerary robotic limbs for aircraft fuselage assembly: body stabilization and guidance by bracing," in *Robotics and Automation (ICRA), 2014 IEEE Int. Conf.*, pp. 1176–1183.
- [11] B. L. Bonilla and H. H. Asada, "A robot on the shoulder: Coordinated human-wearable robot control using coloured petri nets and partial least squares predictions," in *Robotics and Automation (ICRA), 2014 IEEE Int. Conf.*, pp. 119–125.
- [12] J. Mederer. Wearable Robot Transforms Musicians into Three-Armed Drummers [Online]. Available: [Accessed 02-Feb-2017]. <http://www.news.gatech.edu/2016/02/17/wearable-robot-transforms-musicians-three-armed-drummers>.
- [13] F. Wu and H. Asada, "Supernumerary robotic fingers: an alternative upper-limb prosthesis," in *ASME 2014 Dynamic Syst. and Control Conf.*, pp. V002T16A009–V002T16A009.
- [14] I. Hussain, G. Salvietti, M. Malvezzi, and D. Prattichizzo, "Design guidelines for a wearable robotic extra-finger," in *RTSI 2015 IEEE 1st Int. Forum*, pp. 54–60.
- [15] S.-W. Leigh and P. Maes, "Body integrated programmable joints interface," in *Proc. 2016 ACM CHI Conf. Extended Abstracts*, pp. 3719–3722.
- [16] T. Ort, F. Wu, N. C. Hensel, and H. H. Asada, "Supernumerary robotic fingers as a therapeutic device for hemiparetic patients," in *ASME 2015 Dynamic Syst. and Control Conf.*, pp. V002T27A010–V002T27A010.
- [17] Y.-C. Liao, S.-Y. Yang, R.-H. Liang, L. Chan, and B.-Y. Chen, "Thirdhand: wearing a robotic arm to experience rich force feedback," in *SIGGRAPH Asia 2015 Emerging Technologies*. ACM, p. 24.
- [18] L. U. Odhner, R. R. Ma, and A. M. Dollar, "Open-loop precision grasping with underactuated hands inspired by a human manipulation strategy," *IEEE Trans. Autom. Sci. Eng.*, vol. 10, no. 3, pp. 625–633, 2013.
- [19] V. Vatsal and G. Hoffman, "Wearing your arm on your sleeve: Studying usage contexts for a wearable robotic forearm," in *Robot and Human Interactive Communication (RO-MAN), 2017 26th IEEE International Symposium on*. IEEE, 2017.
- [20] R. Hartson and P. S. Pyla, *The UX Book: Process and guidelines for ensuring a quality user experience*. Elsevier, 2012.
- [21] R. S. Hartenberg and J. Denavit, "A kinematic notation for lower pair mechanisms based on matrices," *J. of Appl. Mechanics*, vol. 77, no. 2, pp. 215–221, 1955.
- [22] NASA-STD-3000 Man-System Integration Standards. [Online] Available: [Accessed 02-Feb-2017]. <https://msis.jsc.nasa.gov/>.
- [23] Y. Cao, K. Lu, X. Li, and Y. Zang, "Accurate numerical methods for computing 2d and 3d robot workspace," *Int. J. of Advanced Robotic Syst.*, vol. 8, no. 6, p. 76, 2011.
- [24] ROS.org. Unified Robot Description Format [Online] Available: [Accessed 10-Sep-2017]. <http://wiki.ros.org/urdf>.
- [25] B. Busch. Flowers Laboratory, INRIA. [Online] Available: [Accessed 01-Feb-2017]. [https://github.com/baxterflowers/human\\_moveit\\_config](https://github.com/baxterflowers/human_moveit_config).
- [26] J. Y. Luh, M. W. Walker, and R. P. Paul, "On-line computational scheme for mechanical manipulators," *J. DYN. SYS. MEAS. & CONTR.*, vol. 102, no. 2, pp. 69–76, 1980.
- [27] J. J. Craig, *Introduction to robotics: mechanics and control*. Pearson Prentice Hall Upper Saddle River, 2005, vol. 3.
- [28] K. Kulig, J. G. Andrews, and J. G. Hay, "Human strength curves," *Exercise and sport sciences reviews*, vol. 12, no. 1, pp. 417–466, 1984.
- [29] J. C. Otis, R. F. Warren, S. I. Backus, T. J. Santner, and J. D. Mabrey, "Torque production in the shoulder of the normal young adult male the interaction of function, dominance, joint angle, and angular velocity," *The American J. of Sports Medicine*, vol. 18, no. 2, pp. 119–123, 1990.
- [30] M. Goodrich, D. Olsen, J. Crandall, and T. Palmer, "Experiments in adjustable autonomy," in *Proc. IJCAI Workshop on Autonomy, Delegation and Control: Interacting with Intelligent Agents*. Citeseer, 2001, pp. 1624–1629.
- [31] J. F. Kelley, "An iterative design methodology for user-friendly natural language office information applications," *ACM Transactions on Information Systems (TOIS)*, vol. 2, no. 1, pp. 26–41, 1984.